Establishing a high-accuracy spectral response scale in the near infrared with digital filters

Jarle Gran, Kristian Ellingsberg, and Aasmund S. Sudbø

Spectrally invariant detectors are commonly used to interpolate or extrapolate the responsivity of InGaAs detectors in the infrared from absolute calibrations at a few wavelengths. The random noise in such detectors limits the accuracy that can be achieved in a narrowband, double-monochromator setup. We propose the application of a dedicated digital filter, which reduces the uncertainty by 30%, and combine it by calibrating a group of three detectors. The uncertainties are propagated from the observed variance in the relative measurement to the combined uncertainty of 0.4% (2σ) in the responsivity values of the InGaAs detectors in the range of 1010–1640 nm.

OCIS codes: 120.5630, 120.3940, 040.3060, 040.5160.

1. Introduction

The manufacturing of InGaAs detectors has improved during the past decade[1] and they have become the most popular working standards in the near infrared (NIR). A description of a calibration procedure for infrared standard detectors based on a relative calibration to a spectrally invariant thermal detector and then absolute calibration at a few wavelengths is given by several groups.[2–4] As pointed out in Refs. 2–4, the disadvantage of the thermal detectors is their signal-to-noise ratio when they are used in a narrow-bandwidth double-monochromator setup at room temperature, which limits the accuracy achievable by this method. Because of this problem, the National Institute of Standards and Technology constructed a specially designed cryogenic radiometer in the infrared to eliminate the room-temperature thermal detectors.[5] In our application we use a cavity pyroelectric detector (CPD) as a spectrally invariant detector. Although noisy, the excellent blackness of this detector makes it well suited as a transfer standard in the calibration of InGaAs detectors from known silicon responsivity data.

J. Gran (jarle.gran@justervesent.no) and K. Ellingsberg are with the Norwegian Metrology Service (JV), Fetveien 99, Kjeller N-2007, Norway. A. S. Sudbø is with the University Graduate Center (UniK), University of Oslo, P.O. Box 70, Kjeller N-2007, Norway.

Received 13 May 2004; revised manuscript received 27 September 2004; accepted 1 December 2004.

0003-6935/05/132482-08$15.00/0

We propose to apply a digital filter, designed for the purpose, to reduce the influence of noise on these measurements in the establishment of a spectral response scale. In addition, we propose an algorithm that takes advantage of the known responsivity ratio within a group of several InGaAs detectors to obtain the best estimate of the responsivity from the group. In Section 2 we describe our measurements. The details about the digital filter are given in Section 3, and the data analysis is given in Section 4 including a full covariance analysis where the uncertainty is propagated from the observed variance in the relative measurement. A summary and conclusions are given in Section 5.

2. Measurement of Responsivity

A. Measurement Condition

The relative spectral response was measured in the setup at the Norwegian Metrology Service. This setup consists of a tungsten lamp, a double-grating monochromator, shutter and order-sorting filters, a detector translation stage, and readout electronics. In addition, input and output optics of the monochromator consists of reflection optics, assuring no spectral dependence when the beam is imaged onto the detectors. The monochromator output slit used in the measurements was 1 mm, giving a spectral width of 4 nm. The signals from the two detectors were amplified and read by a digital voltmeter. The whole system is computer controlled and fully automated.

The relative spectral response of the InGaAs detectors was measured with the CPD purchased from National Physical Laboratory, UK, as a spectrally

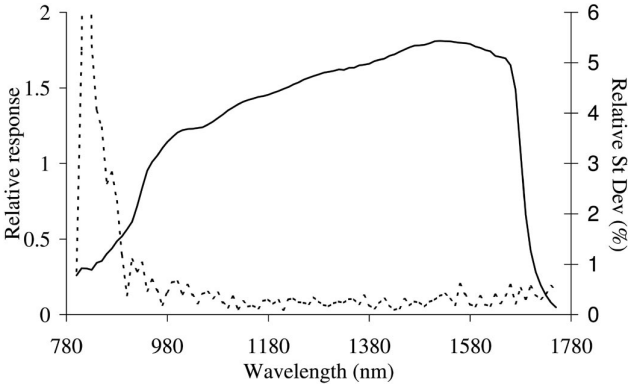

Fig. 1. Relative spectral response measured against a CPD and the corresponding standard deviation for one of the three InGaAs detectors.

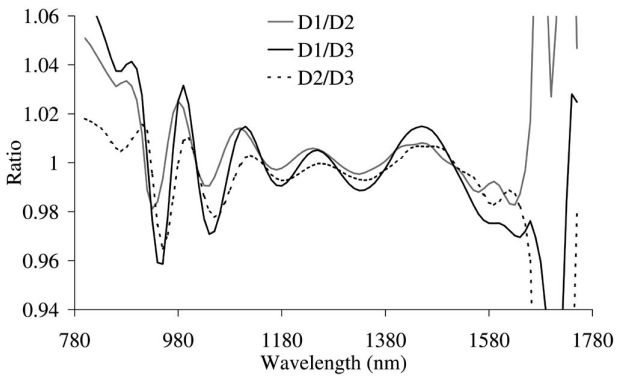

Fig. 2. Spectral responsivity ratios between the three InGaAs detectors.

invariant detector.[2] This detector has an active element with a platinum black coating inside an aluminum reflective hemisphere. The CPD needs a preamplifier, a chopper, and a lock-in amplifier to give a dc-equivalent signal. The chopper was frequency locked to 75 Hz with a typical short-term (compared with the measurement integration time of the CPD) instability of ± 0.02 Hz. At a chopper frequency of 75 Hz, the CPD response has a frequency sensitivity of $-0.6\%/\text{Hz}$, resulting in a contribution of 0.012% to the standard deviation at each point. This uncertainty contribution is further reduced by averaging, since the fluctuations are rapid compared to the measurement integration time. This assures that there is no additional uncertainty in the relative measurements due to the frequency dependence in the detection process made by the CPD. The InGaAs detectors have a 5-mm-diameter active element and were manufactured by Germanium Power Devices Model GAP5001. We measured each of the three detectors twice, with a 10-nm wavelength spacing in the spectral range from 800 to 1750 nm, for a total of six series. The temperature in the laboratory was 23 °C $\pm$ 0.5 °C and the relative humidity was 45 $\pm$ 5%.

B. Measurement Procedure

Our goal is to calibrate a group of three detectors to establish a spectral response scale in the NIR. These detectors will be used to calibrate other detectors in the same spectral range. There are several measurements needed to achieve this calibration. First we make a relative measurement between each of the InGaAs detectors and the CPD over the spectral range. This gives us the relative spectral response of all three InGaAs detectors. The average values of one InGaAs detector and its relative standard deviations are shown in Fig. 1, as an example. The uncertainty is dominated by the typical random noise from the CPD in these measurements.

The individual response ratios between the InGaAs detectors, without the CPD, are measured over the whole spectral range. This gives us information about the actual responsivity ratio between the detectors, with low type A uncertainty, when they are measured under the same environmental conditions. Type A uncertainty is the common term for the uncertainty evaluated by statistical methods, often as the observed standard deviation in an experiment. In contrast, type B uncertainty is evaluated by other means. These ratios are shown in Fig. 2.

After performing the relative measurements, we make an absolute calibration at a few wavelengths in the range of 800–1000 nm against an accurate silicon trap detector. This measurement could be done for all detectors at the same time, because the type A uncertainty in this measurement is negligible compared with the relative measurements. We need this measurement to scale the relative measurement to absolute responsivities.

We denote our InGaAs detectors by D1, D2, and D3. The measurements were performed at different time and gain settings for the detectors. The relative measurement of D2 was made with the amplifier gain reduced by a factor of 10, and the relative measurement of detector D1 was performed several months after the other two measurements, as the initial measurement was found to be inconsistent with the other two. We found the error by comparing the relative measurements of the detectors to the low-noise reference ratios. A slope in the ratios caused by the relative measurement of D1 was observed. The remeasured data were found to be satisfactory, showing that the measurement procedure presented here is robust.

The measurement time for the ratio measurements between the InGaAs detectors is only a few hours, whereas the total measurement time for the six calibration series against the CPD was approximately 24 h. The result of the long measurement time is that some of the typical environmental changes are included in the observed variance of the relative measurements. Measuring three different detectors is not expected to improve the uncertainty estimate of the group instead of our using the same amount of measurements on one detector. But basing the spectral response scale on one detector only is not satisfactory; and by the changing grating and the detectors, systematic errors will appear in the observed variance of

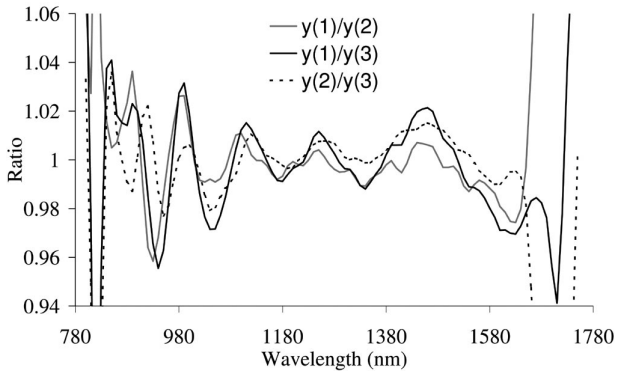

Fig. 3. Ratios of the relative spectral response of the three InGaAs detectors, each measured against the CPD, for one randomly chosen series.

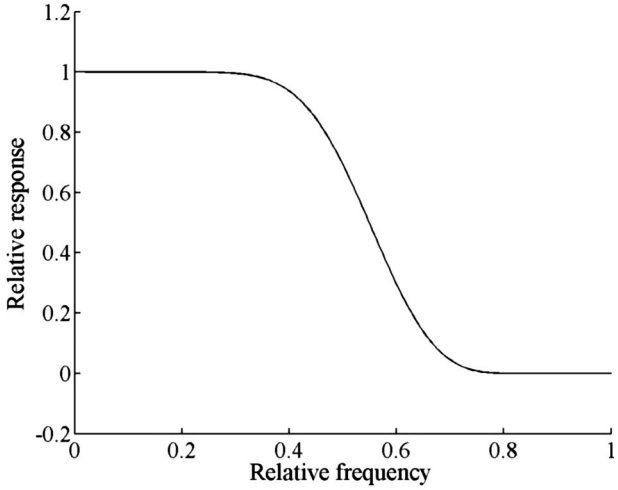

Fig. 4. Frequency response of the digital filter in terms of sampling frequency shown in a linear scale. The frequency is given between 0 and f_b, where f_b is half of the sampling frequency ($f_s/2$).

the group. In addition, we have the ability of making consistency tests on the data, and we still use all measurements within the group to establish the responsivity scale.

C. Measurement Results

The six different measurement series were treated separately through the calculations because this gives us the ability to measure consistency between the uncertainty calculation and the observed variance in the final responsivity values. In Fig. 3 we show the responsivity ratios for one arbitrarily chosen measurement series, and it is clear that this ratio has more noise than the ratio between two InGaAs detectors measured directly without involving the CPD. Because of the low monochromator throughput at the shortest wavelengths, we have a large standard deviation, as can be seen in Fig. 1.

3. Design and Application of a Digital Filter

The spectral responsivity of an InGaAs detector, as shown in Fig. 1, can be regarded as the response of a continuous time signal. The responsivity at one wavelength depends on the neighboring wavelengths because the true responsivity of the detectors varies smoothly with wavelength. This enables us to apply a dedicated digital filter to reduce the noise in the relative spectral response measurements.

A. Filter Design

The desired responsivity of the filter, when we regard the responsivity as a signal response, is that high-frequency components (sample-to-sample variance) should be rejected whereas the true variations in the signal are passed through undistorted. To define the desired frequency cutoff band, we used the signal ratios of Fig. 2 as the reference to determine the maximum signal frequency (in terms of sampling frequency f_s) that should pass through undistorted. We therefore introduce a frequency f defined in the frequency band $0 \leq f \leq f_b$, where f_b equals half of the sampling frequency ($f_s/2$). The highest signal period observed is ten samples in the short-wavelength range (890–990 nm), which is equivalent to $0.2f_b$. It is important that this frequency and the frequency components in the slope around 920 nm pass through undistorted so that the filter does not introduce any error.

We chose to use a Chebyshev low-pass filter on the data. This filter is a symmetric low-pass finite impulse response filter with a flat monotonically decreasing passband and an equiripple stop band. Its taps are calculated by the MATLAB program cheblp2 (Ref. 6) with input parameters N (filter width, in number of taps) equal to 19, L (degree of flatness at $f = 0$) equal to 12, and w_s (the stop band edge) set to 0.8. This yields the frequency response shown in Fig. 4 for frequencies between 0 and f_b. The filter response decreases smoothly from 1 at dc to 0.999 at $0.27\,f_b$. From there the rejection increases rapidly down to 0.0001 at $0.8\,f_b$.

B. Resulting Filter

The application of a digital filter gives a new smoothed value at one wavelength from its original value at that wavelength and its neighboring values by applying different weights on those values. To maintain the dc value, the sum of the weights is equal to 1. The calculated weights for our filter with a filter width of 19 taps are shown in Fig. 5. To obtain the desired frequency response, some of the weights are negative.

To calculate all values and uncertainties in one operation, the weight vector in Fig. 5 was used to form a filter matrix **W**. In both ends of the measurement vector we cannot use all components of the filter to produce new estimates. We chose to keep the symmetry of the filter in both ends of the measurement vector and used the normalized subset of the central part (wavelength λ in Fig. 5) of the filter vector. This means that the first and last sample points are unfiltered and the second from both ends are filtered from its original value and the neighboring values on both sides only. This procedure is repeated by in-

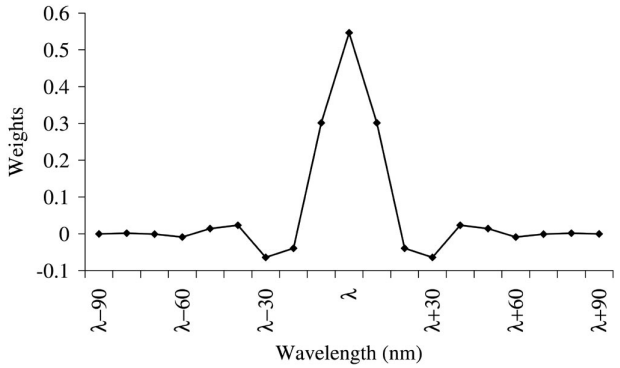

Fig. 5. Weights of the digital filter. The wavelengths are given as the relative position to the sample point filtered with a sampling interval of 10 nm.

creasing the filter width until sample point 10 (890 nm), where we apply the full width of the filter. This is not a problem since we will use the values where we can apply the full filter width in our calculations, so the special case in the ends is introduced to simplify the calculations. The filter we use is expected to reduce the variance with 50%, which is equivalent to a reduction in the relative standard deviation by 30% at each sample point.

4. Calculation of Responsivity and Uncertainty

To estimate the responsivity of the detectors, our procedure includes a couple of steps. These steps are handled separately in the following subsections. In Fig. 6 we show a flow diagram of the realization chain to make it easier to follow the steps needed to find the absolute response of the InGaAs detectors.

A. Convert Data onto One Detector

We want to base our scale on a group of three detectors. To obtain a consistent set of the responsivity from the group, we use the measured responsivity ratios between each of the InGaAs detectors and D1 to convert the measured spectral response of each of the two other detectors to an independently measured spectral response of detector D1. This enables us to use the measurements of all three detectors in the estimate of the spectral response of one detector. If the uncertainty is dominated by type A uncertainty in the calibration against the CPD, this is equivalent to measuring detector D1 three times. Because the relative response scaling constant is in general different for the three detectors, for example, because of realignment of the optics, we have to find the constant needed to convert one detector onto another. This is done by fitting the ratio of the filtered data to the known responsivity ratios given in Fig. 2 with a constant. To do so we start by filtering the relative response of all detectors. This is found as

$$\bar{\mathbf{y}}(m) = \mathbf{W}\mathbf{y}(m), \tag{1}$$

where $y(m)_i$ is the relative response measured at wavelength λ_i, $W_{i,j}$ is the filter transfer function, and

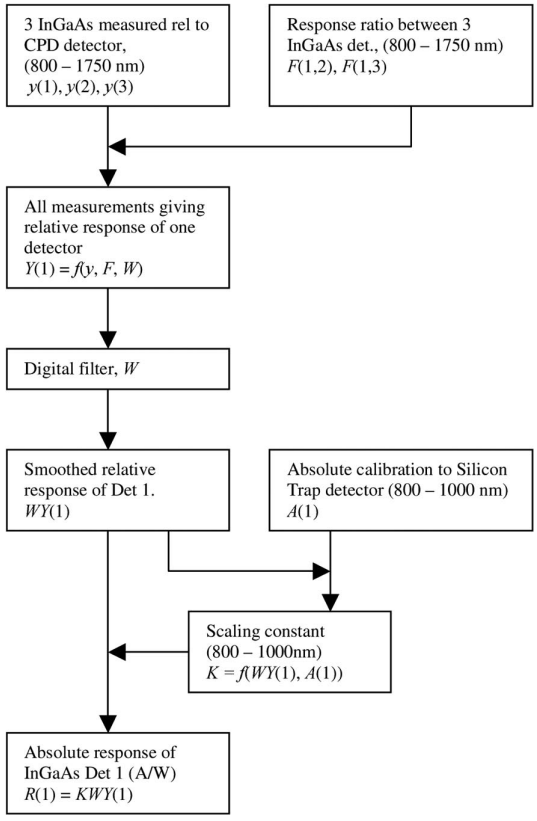

Fig. 6. Flow diagram showing the principles in the realization of the spectral response scale.

$\bar{y}(m)_i$ is the corresponding filtered relative response of the detector. m is the index identifying the detector $m = 1, 2$, or 3. The detectors were measured at N wavelengths λ_i. The covariance matrix of $\bar{\mathbf{y}}(m)$ is[7]

$$\mathbf{u}^{(\bar{\mathbf{y}})}(m) = \mathbf{W}\mathbf{u}^{(\mathbf{y})}(m)\mathbf{W}^T, \tag{2}$$

where the variance in the observed data $\mathbf{y}(m)$ is given as the diagonal matrix $\mathbf{u}^{(\mathbf{y})}(m)$ calculated from the six series of the relative measurements for that detector. $\mathbf{W}$ has the same meaning as in Eq. (1). The filter we use is expected to reduce the variance with 50%, simply calculated with a unitary diagonal matrix as the input variance. This is equivalent to a 30% reduction in the relative standard deviation at each sample point.

The second step in the conversion of measurements of one detector onto another is to find the scaling constant between the detectors, caused by the fact that the detectors were realigned with different optical configurations and gain settings. We do this by calculating the average constant between the directly measured ratios between the detectors and the ratios between the smoothed relative data. This is expressed mathematically as

$$a(m) = \frac{1}{(N-n+1)} \sum_{i=n}^{N} \frac{F(1,\, m)_i}{r(1,\, m)_i}, \tag{3}$$

where $F(1, m)_i$ are the vector elements in the measured ratio between detector D1 and m at λ_i, (shown in Fig. 2) and $r(1, m)_i = \bar{y}(1)_i/\bar{y}(m)_i$. N is the index of the last element and n is the index of the starting element. Because of the large standard deviation for the shortest wavelengths in the relative measurement to the CPD (as can be seen in Fig. 1), we excluded them in the calculation of the scaling constant.

The six series were treated separately through all our calculations. The scaling constants $a(m)$ were calculated and used separately for all series to obtain an average value of detector D1 from the converted data by

$$Y(1)_i = \frac{1}{3}\left[y(1)_i + \frac{1}{a(2)}\, y(2)_i F(1,\ 2)_i + \frac{1}{a(3)}\, y(3)_i F(1,\ 3)_i\right]. \tag{4}$$

In this way all detectors are equally weighted in the establishment of the spectral response scale. All detectors are the standard detector. To use all measurements within the group we have to convert the other two detectors onto one of them as done in Eq. (4). The variance of the converted data could be calculated from the input variance of each sample point only. But we chose to calculate a new variance matrix from the observed variance between each of the measurement series of the combined set of data instead, because this will include the uncertainty in the conversion and the systematic effects from the fact that measurements were done with a different alignment, a new grating, and wavelength calibration. We achieved an average value of all three detectors in each series mapped onto detector D1 with an associated uncertainty $\mathbf{u}^{(\mathbf{Y})}$, which is greater than the observed variance of one detector divided by 3.

B. Making the Relative Measurement Absolute

To find the absolute responsivities of the detectors we apply our digital filter on the converted data and then scale them by comparing the filtered relative data to the absolute calibrated data of detector D1. The responsivity of D1 is calculated by fitting $\mathbf{WY}(1)$ to $\mathbf{A}(1)$ by a scaling constant K as

$$\mathbf{R}(1) = K\mathbf{WY}(1). \tag{5}$$

The scaling constant K is calculated from the points where we have good estimates of the responsivity from the calibration to the silicon trap detector (800–1000 nm) and is calculated from the absolute calibration and the filtered relative response as

$$K = \frac{1}{(M - n + 1)} \sum_{i=n}^{M} \frac{A(1)_i}{[WY(1)]_i}, \tag{6}$$

where $A(1)_i$ is the absolute response of D1 at wavelength λ_i and $Y(1)_i$ is given in Eq. (4). M is the length of the vector $\mathbf{A}(1)$, measured between 800 and 1000 nm. We introduced the value n as the index for the starting wavelength in the calculation of K because the values of $Y(1)_i$ have too high an uncertainty for the shortest wavelengths (see Fig. 1); using them in the calculation of the average value actually introduces a higher uncertainty than omitting them.

To find the uncertainty in the responsivity given in Eq. (5), we have to calculate the uncertainty in the scaling constant and the uncertainty in the filtered relative data. The uncertainty in the scaling constant is calculated by differentiating Eq. (6) with respect to both filtered data and absolute calibrated data. To perform this calculation it is advantageous to expand the length of vector $\mathbf{A}(1)$ to have the same length as $\mathbf{Y}(1)$. This is done by adding zeros to $\mathbf{A}(1)$ for all elements between M and N and for elements below n. If we do this we can let the sum in Eq. (6) to go from 1 to N without changing the value of K. The normalization constant in front of the summation sign is kept unchanged. In addition, the uncertainty elements of the absolute calibration $[\mathbf{u}^{(\mathbf{A})}]$ from M to N is set to zero. This means that all the sensitivity vectors have the length N and the input uncertainty matrix has the dimension $N \times N$. This gives us the following uncertainty in the scaling constant expressed by input uncertainties as

$$\mathbf{u}^{(K)} = \mathbf{\Psi}\mathbf{W}\mathbf{u}^{(\mathbf{Y})}\mathbf{W}^T\mathbf{\Psi}^T + \mathbf{a}\mathbf{u}^{(\mathbf{A})}\boldsymbol{\alpha}^T, \tag{7}$$

where $\mathbf{\Psi}$ is the row vector of sensitivity coefficients of K in Eq. (6) with respect on the converted filtered data $\mathbf{WY}(1)$ and the weights above M and below n is zero. The matrix $\mathbf{W}\mathbf{u}^{(\mathbf{Y})}\mathbf{W}^T$ is the covariance matrix of the converted filtered data. $\boldsymbol{\alpha}$ is the row vector of sensitivity coefficients of K with respect to the absolute calibration from the silicon trap detector with uncertainty $\mathbf{u}^{(\mathbf{A})}$. A value for n between 9 and 16 (corresponding to a wavelength λ between 880 and 950 nm) gave the lowest uncertainty in the scaling constant for the series, and the differences in uncertainty for n within this range were negligible.

After calculating the uncertainty in the scaling constant K, we can calculate the uncertainty in the responsivity, given in Eq. (5), by differentiating it with respect to the filtered converted data and the uncertainty in the scaling constant as

$$\mathbf{u}^{(\mathbf{R})} = K^2\mathbf{W}\mathbf{u}^{(\mathbf{Y})}\mathbf{W}^T + [\mathbf{WY}(1)]\mathbf{u}^{(K)}[\mathbf{WY}(1)]^T, \tag{8}$$

where $\mathbf{u}^{(\mathbf{R})}$ is a $N \times N$ covariance matrix for the responsivity of D1. The responsivity values are correlated through the filter and the scaling constant and are calculated from the observed variance in each sample point. The correlation matrix calculated from Eq. (8) is shown in Fig. 7. Figure 7 clearly shows the correlation caused by the filter and the scaling constant, as Gardner[8] showed in his paper. The ridge along the matrix diagonal shows the correlation caused by the filter. The width of the ridge is determined by the width of the filter shown in Fig. 5. The

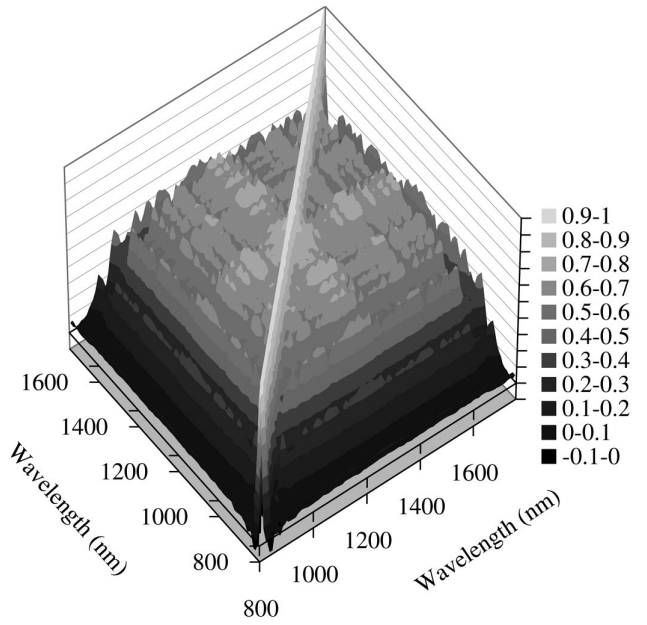

Fig. 7. Calculated correlation matrix for the responsivity values at different wavelengths. The ridge along the diagonal appears from the filter, and the broad spectral correlation coefficient is caused by the uncertainty in the scaling constant.

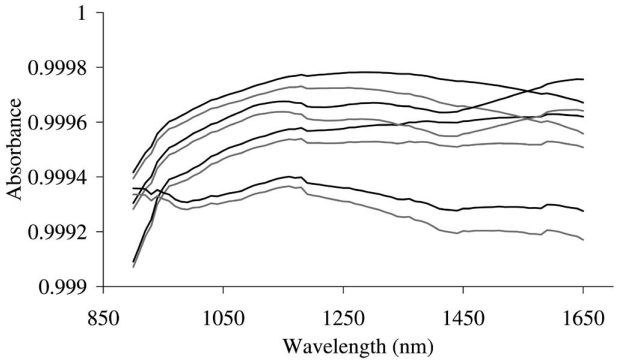

Fig. 8. Estimated spectral dependence of the CPD for four different sets of reflectance data of UV-enhanced aluminum. The black curves are for the case in which the radiation undergoes two reflections on the aluminum-coated hemisphere, whereas the gray curves are calculated for the case in which the radiation undergoes one reflection at the hemisphere.

broad correlation coefficients are caused by the uncertainty in the scaling constant in Eq. (7) and shows that it plays a significant role in the total uncertainty.

C. Uncertainty Components

The different uncertainty components are listed in Table 1. Those values treated as spectrally invariant—linearity, uniformity, stray light, and electrical calibration of an amplifier and digital voltmeter—are given a numerical value in Table 1.

One of the essential properties in this method is the assumed spectral invariance of the CPD. The spectral reflectance of the pyroelectric element was measured by the same method as Gran and Sudbø[9] in the visual part of the spectrum. But because our measurement could not be made absolute, we had to scale the diffuse reflectance to fit the reflectance values in the previously mentioned reference. To estimate the spectral dependence of the CPD we have to take into account the reflectance of the UV-enhanced aluminum coating on the reflective hemisphere. The detector is designed to absorb radiation that undergoes at least two reflections from the hemisphere before it leaves the detector. The CPD absorbance for four different sets of aluminum reflectance data is given in Fig. 8. We calculated the absorbance under the assumption that the radiation undergoes one and two reflections for each set of reflectance data. The data between 900 and 920 nm are based on three silicon detectors surrounding the active element, and the rest of the data are based on measurements with the InGaAs detector. Figure 8 shows that it is not reliable to correct for the spectral dependence of the aluminum reflectance. But Fig. 8 also shows that the spectral difference from maximum to minimum absorbance is less than 0.06%, independent of the data used and independent of the number of reflections the radiation undergoes. We therefore chose to treat the uncertainty as spectrally invariant with a value of 0.06% in Table 1.

The diagonal elements in Eq. (8) give the type A

Table 1. Accounted Uncertainty Components in the Estimated Responsivity

Source of Uncertainty	Comment	Relative Uncertainty in Responsivity (%)
Type A	Spectrally dependent	Fig. 9
Temperature (0.5 °C)	Spectrally dependent	Fig. 9
Wavelength (0.2 nm)	Spectrally dependent	Fig. 9
Uniformity of InGaAs detectors		0.1
Uniformity of CPD		0.05
Stray light		0.03
CPD nonblackness	Fig. 8	0.06
Nonlinearity of InGaAs detector		<0.001
Electrical calibration	Amplifier and digital voltmeter	0.02
Absolute calibration to silicon trap detector	(0.1%–0.25%), contributes to the type A uncertainty in Eqs. (8)–(7)	
Combined standard uncertainty	Spectrally dependent	Fig. 9

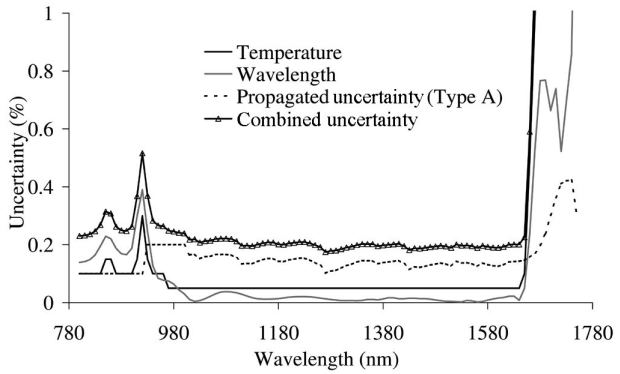

Fig. 9. Spectral dependent uncertainty components for each of the measurement series in the establishment of a spectral response scale in the infrared, in addition to the combined uncertainty of all components. The uncertainties are given with a 1σ level of confidence.

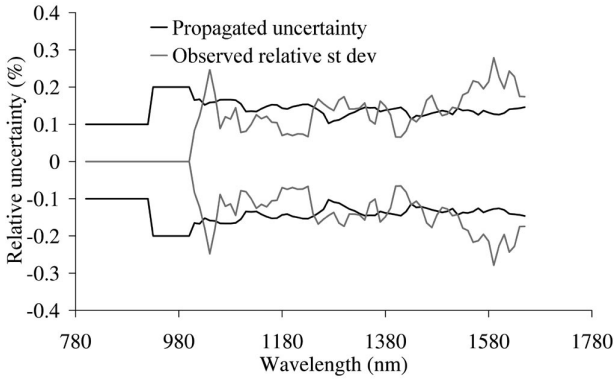

Fig. 10. Comparison of the propagated type A uncertainty and the observed standard deviation in the calculated responsivity values over the spectral range where the type A uncertainty is the dominating uncertainty component. The uncertainties are given with a 1σ level of confidence.

uncertainty for each of the series in the responsivity values of D1. The different spectrally dependent uncertainty components and the combined standard uncertainty are shown in Fig. 9.

The temperature-related uncertainty was studied by Fox,[1] Werner *et al.*,[4] and Shaw *et al.*[5] for this kind of detector. It shows that the uncertainty in responsivity due to temperature is approximately equal to or less than 0.05% for the spectral range from 950 to 1640 nm. From 1640 to 1700 nm there is a large increase in temperature sensitivity due to the bandgap edge of InGaAs to approximately 2.5% with our laboratory conditions. For shorter wavelengths the uncertainties are a little different for these references. Werner *et al.* report the highest uncertainty, which is approximately 0.6%/°C around 925 nm, and this corresponds to an uncertainty of 0.3% in our laboratory. At other wavelengths the temperature-induced uncertainty is less than 0.1%/°C. Because the measurements were made over several days and then combined, some variations in the results because of temperature variations appear as type A uncertainty.

The uncertainty associated with linearity is spectrally dependent. Fox[1] shows that the detector was supralinear at short wavelengths (<960 nm) caused by absorption sites inside the InP cap layer. The increase in responsivity with optical power was changing linearly with almost 1% over 3 decades of optical power, from 0.1 μW to 0.1 mW. This would result in an uncertainty due to linearity in our application to approximately 0.001% at 850 nm. The nonlinearity at longer wavelengths (1550 nm) is less than 0.1% for all power levels up to 0.2 mW and hardly detectable below 20 μW. In our application the nonlinearity contribution to the uncertainty is negligible.

The uncertainty due to wavelength is calculated from the numerical derivative of the responsivity with an uncertainty in the wavelength of 0.2 nm, which is the accuracy of the monochromator. The nonuniformity of the InGaAs detectors with a 3-mm spot size is evaluated, from a small spot at a 1300-nm raster scan, to be 0.1%. The presented method shows the calculated uncertainty including the transfer from the known silicon values and their estimated uncertainty. The combined standard uncertainty is also shown in Fig. 9.

As a control of our uncertainty calculation, a comparison between the average propagated uncertainty and the observed relative standard deviation in the responsivity values for the six series are shown in Fig. 10. These are two different ways to calculate the type A uncertainties in the measurements. The propagated uncertainty is based on the observed variance of the relative measurements, and the observed standard deviation is based on the standard deviation in the calculated absolute responsivity. The two uncertainty estimates should be equal in the type A limiting range, and the observed agreement in Fig. 10 confirms our uncertainty calculation.

5. Summary and Conclusions

We have established a high-accuracy spectral response scale in the NIR based on three InGaAs detectors by measuring the relative response of each of them with a CPD. These three detectors will then define the spectral response scale at the Norwegian Metrology Service. To reduce the influence of the dominating random noise from the CPD, we apply a digital short-pass filter designed for this purpose. This reduces the standard deviation in our measurements by 30%. We found the responsivity ratios between the detectors by measuring their responses against each other under the same environmental conditions without the noisy CPD. This measurement was used to convert the measurements of detector D2 and D3 onto detector D1 and thus obtain the equivalent of the average value from the group. It was also used to check the consistency in the relative measurements of the detectors and assure the integrity of each individual detector as a calibration reference. The converted relative data were filtered and scaled to produce the absolute responsivity, whereas its covariance matrix was calculated from the observed

variance in the relative data directly. The filter reduces the propagated uncertainty in the responsivity, which limits the accuracy in the central part of the spectrum. Wavelength and temperature-related uncertainties limit the accuracy in the ends of the spectrum. With the present setup we have established a spectral response scale in the NIR, based on three different InGaAs detectors, with 0.4% relative uncertainty (95% level of confidence) over the spectral region from 1000 to 1640 nm. This accuracy is comparable to the 0.37% given by the National Physical Laboratory.[3]

References

1. N. P. Fox, "Improved near-infrared detectors," Metrologia **30,** 321–325 (1993).
2. D. H. Nettleton, T. R. Prior, and T. H. Ward, "Improved spectral responsivity scales at the NPL, 400 nm to 20 μm," Metrologia **30,** 425–432 (1993).
3. N. P. Fox, E. Theocharous, and T. H. Ward, "Establishing a new ultraviolet and near-infrared spectral responsivity scale," Metrologia **35,** 535–541 (1998).
4. L. Werner, R. Friedrich, U. Johannsen, and A. Steiger, "Precise scale of spectral responsivity for InGaAs detectors based on a cryogenic radiometer and several laser sources," Metrologia **37,** 523–526 (2000).
5. P. S. Shaw, T. C. Larason, R. Gupta, S. W. Brown, and K. R. Lykke, "Improved near-infrared spectral responsivity scale," J. Res. Natl. Stand. Technol. **105,** 689–700 (2000).
6. I. W. Selesnick and C. S. Burrus, "Exchange algorithms for the design of linear phase FIR filters and differentiators having flat monotonic passbands and equiripple stopbands," IEEE Trans. Circuits Syst. II **43,** 671–675 (1996).
7. International Organization for Standardization, "Guide to the expression of uncertainty in measurement," (ISO, Geneva, 1993), Eq. H.9 in matrix form, p. 72.
8. J. L. Gardner, "Correlations in primary spectral standards," Metrologia **40,** S167–S171 (2003).
9. J. Gran and A. S. Sudbø, "Absolute calibration of silicon photodiodes by purely relative measurements," Metrologia **41,** 204–212 (2004).